

Ytterbium Complexes with Chlorin e_6 Derivatives for Targeted NIR-II Bioimaging

Alexander A. Popov,^{a@1} Nikita V. Suvorov,^a Andrey I. Kornikov,^b Petr V. Ostroverkhov,^a Sergey I. Tikhonov,^a Viktor A. Pogorilyy,^a Anastasia I. Demina,^a Maxim N. Usachev,^a Ekaterina A. Plotnikova,^{a,c} Andrey A. Pankratov,^{a,c} Leonid S. Lepnev,^d Elnara S. Saffiulina,^e Valentina V. Utochnikova,^{b@2} Elena R. Milaeva,^b and Mikhail A. Grin^{a@3}

^aDepartment of Chemistry and Technology of Biologically Active Compounds, Medicinal and Organic Chemistry, Institute of Fine Chemical Technologies, MIREA – Russian Technological University, 119571 Moscow, Russia

^bDepartment of Chemistry, M.V. Lomonosov Moscow State University, 119991 Moscow, Russia

^cP. Hertsen Moscow Oncology Research Institute – Branch of the National Medical Research Radiological Centre of the Ministry of Health of Russian Federation, 125284 Moscow, Russia

^dP.N. Lebedev Physical Institute of the Russian Academy of Sciences, 119991 Moscow, Russia

^eA.N. Nesmeyanov Institute of Organoelement Compounds of the Russian Academy of Science, 119334 Moscow, Russia

^{@1}Corresponding author E-mail: alexander.p.tmb@gmail.com

^{@2}Corresponding author E-mail: valentina.utochnikova@gmail.com

^{@3}Corresponding author E-mail: michael_grin@mail.ru

Two novel chlorin e_6 derivatives containing chelating groups on the periphery of the macrocycle were obtained, and two novel complexes of ytterbium with these chlorins were synthesized and characterized. It was found that NIR-II emission of Yb ion was sensitized by chlorins, the sensitization efficiency depended on the distance from Yb to chlorin core. The detailed study of ytterbium complexes luminescence and *in vitro* experiments were carried out, during which the kinetics of accumulation in tumor cells have been studied. Due to their properties, the obtained metal complexes could find potential application in fluorescent imaging in the NIR-II range.

Keywords: Natural chlorins, luminescence, NIR-II, chelators, ytterbium, chlorophyll *a*, carboxylate complexes, lanthanides.

Иттербиевые комплексы производных хлорина e_6 для таргетной NIR-II биовизуализации

А. А. Попов,^{a@1} Н. В. Суворов,^a А. И. Корников,^b П. В. Островерхов,^a С. И. Тихонов,^a В. А. Погорилый,^a А. И. Демина,^a М. Н. Усачев,^a Е. А. Плотникова,^{a,c} А. А. Панкратов,^{a,c} Л. С. Лепнев,^d Э. С. Сафиуллина,^e В. В. Уточникова,^{b@2} Е. Р. Милаева,^b М. А. Грин^{a@3}

^aКафедра химии и технологии биологически активных соединений, медицинской и органической химии, Институт тонких химических технологий им. М.В. Ломоносова, МИРЭА – Российский технологический университет, 119571 Москва, Россия

^bХимический факультет, Московский государственный институт им. М.В. Ломоносова, 119991 Москва, Россия

^cМосковский научно-исследовательский онкологический институт имени П.А. Герцена – филиал ФГБУ «НМИЦ радиологии» Минздрава России, 125284 Москва, Россия

^dФизический институт им. П.Н. Лебедева РАН, 119991 Москва, Россия

^eИнститут элементоорганических соединений им. А. Н. Несмеянова РАН, 119334 Москва, Россия

^{@1}E-mail: alexander.p.tmb@gmail.com

^{@2}E-mail: valentina.utochnikova@gmail.com

^{@3}E-mail: michael_grin@mail.ru

Получены два новых производных хлорина *e₆*, содержащих хелатирующие группы на периферии макроцикла, а также были синтезированы и охарактеризованы их комплексы с иттербием. Обнаружено, что излучение иона иттербия в ближней инфракрасной области II (NIR-II) сенсibilizировалось хлоринами, при этом эффективность сенсibilизации зависела от расстояния между атомом Yb и хлориновым ядром. Проведены детальные исследования люминесценции комплексов иттербия и эксперименты *in vitro*, в ходе которых изучена кинетика накопления в опухолевых клетках. Благодаря своим свойствам полученные металлокомплексы могут найти потенциальное применение в флуоресцентной визуализации в NIR-II диапазоне.

Ключевые слова: Природные хлорины, люминесценция, NIR-II, хелаторы, иттербий, хлорофилл *a*, карбоксилатные комплексы, лантаноиды.

Introduction

Diagnosing cancer in the early stages is a very important task of modern medicine and a key challenge faced by scientists from all over the world. The diagnosis and treatment of cancer is requiring individualized approaches,^[1] which, in turn, necessitate highly contrasted, real-time bioimages. Non-invasive methodologies are required in order to perturb the investigated systems and organs as little as possible, and optical emissive probes are emerging as strong candidates for this purpose, and especially luminescent bioprobes.^[2] Indeed, when appropriate wavelengths are used, penetration depth may be substantial, and light can reach regions of complex molecular edifices which are not accessible to other molecular probes. In addition, the emitted photons are easily detected by highly sensitive devices and techniques, including single-photon detection.^[3]

However, to create an effective bioimaging agent, two requirements must be met: firstly, the bioprobe with targeting ability and selectivity is required,^[4] and secondly, the penetration depth must be remarkable. The latter hampers the application of the most of the conventional luminescent sensors, which is only suitable for skin and external tissues diagnosing. In order to solve these problems, it is necessary to obtain the NIR-II emitter, whose emission wavelength would coincide with the transparency window of biological tissues, as well as ensure its vector properties.^[5–7]

Ytterbium ion is one of the most prospective candidates for biological applications due to its unique optical properties, which include narrow luminescence bands, providing almost monochromatic emission, and their constant position.^[8–11] There are some other unsurpassed advantages of ytterbium luminescence: 1) being within the NIR-II region ($\lambda_{\max} = 978$ nm), it perfectly fits into the transparency window of biological tissues;^[12,13] 2) large Stokes shift (up to hundreds of nm), incomparable to other classes of bioprobes,^[14,15] allows exciting and emitted light separation; 3) typical narrow emission bands can be easily detected and do not overlap (in contrast to the broad bands of organic molecules).^[16–19]

However, the absorption of ytterbium ions is low, and for effective luminescence of ytterbium an antenna, able to efficiently absorb energy and transfer it to the ytterbium, is needed.^[20] In addition, a specific requirement for ytterbium compounds as bioprobes is the polydentate nature of the ligand to ensure strong chelation and to avoid the complex dissociation.^[21,22] The best Yb sensitizers were found among porphyrins,^[23–25] phthalocyanines,^[26–28] Schiff bases,^[10,29–32] and aromatic carboxylates.^[8,33,34]

Among the compounds with the efficient targeting ability, both small molecules (folic acid, carbohydrates, peptides, *etc.*) and high molecular weight compounds (monoclonal antibodies, vector proteins, nanomaterials, *etc.*) were proposed.^[35–42] Some of the substances that have an increased tropism for tumors are compounds of tetrapyrrole nature, which include phthalocyanines and porphyrins, as well as their hydrogenated analogues. Among them, a special place is occupied by chlorophyll *a* derivatives, which have high availability and abundance in natural raw materials, as well as excellent photophysical properties. Due to their ability to generate reactive oxygen species when irradiated with light in the near-infrared region, as well as the ability to better accumulate in tumor tissues compared to normal ones, they have found their use in photodynamic therapy of oncological diseases as drugs.^[43–46] In addition, chlorins are promising materials for application in luminescence bioprobes, in particular as ligands for lanthanide luminescence. Chlorins are derivatives of porphyrins, which are the effective sensitizers of ytterbium luminescence, so we can expect them to feature the antenna properties and efficient transfer of excitation to central ion. Porphyrins absorption bands are in the red region,^[47,48] which will allow porphyrin-based biotags to absorb light not only in the external tissues of the body. Besides, the vast possibilities for the deliberate design of the chlorin molecules make it possible to add plenty carboxyl groups to the ligand structure. This allows us to achieve coordination not only in the tetrapyrrole coordination sphere, but also due to the chelation by the carboxyl groups – this type of coordination is well known for ligands such as EDTA, DTPA, DOTA and DO3A.^[49–52]

Thus, in the present work, we aim to deliberately obtain chlorins, containing four carboxy-groups that can strongly chelate ytterbium, and to obtain dual (Vis and NIR-II) emissive ytterbium complexes. Their luminescent properties, as well as cell penetration, was studied in comparison with that of the initial chlorins. As part of this work, we intend to answer two important questions: whether the resulting chlorins sensitize the luminescence of ytterbium, despite the large aliphatic fragment, and whether the vector properties of chlorins are preserved during the complex formation.

Experimental

General

All the chemicals were obtained from commercial sources (Merck KGaA, Darmstadt, Germany; Acros Organics – part of Thermo Fischer Scientific, Waltham, MA, USA). Silica gel 60

(Merck KGaA, Darmstadt, Germany) was used for column chromatography. Analytical TLC was performed on aluminum plates with F₂₅₄ silica gel 60 (Merck KGaA, Darmstadt, Germany). ESI-LCMS data were recorded on Agilent 6160 (Agilent, Singapore) with electrospray ionization either in a positive or negative mode. NMR spectra were obtained on a Bruker DPX300 spectrometer (Bruker Corporation, Billerica, MA, USA) using CDCl₃ and DMSO- d_6 as solvents. Residual solvent was used as the reference standard for spectra calibrating. MALDI mass spectra (positively charged ion detection mode) were recorded on a Bruker autoflex speed mass spectrometer (Bruker Daltonics Inc., Germany) equipped with a solid-state UV laser ($\lambda = 355$ nm) and a reflectron, at the lowest possible laser energy (usually 50% from maximum). To record MALDI mass spectra, an MTP 384 ground steel target (Bruker Daltonics Inc., Germany) was used. The analytes solutions in tetrahydrofuran (2 mg/mL) were mixed with the solution of the matrix compound (*trans*-2-[3-(4-*tert*-butylphenyl)-2-methyl-2-propenylidene]malononitrile) in tetrahydrofuran (30 mg/mL) in 1:1 ratio, the mixture was applied to the target and air-dried. Emission and excitation spectra in the visible range were measured using a FluoroMax Plus spectrophotometer (Horiba Ltd., Japan) equipped with a 150 W Ozone-free xenon arc lamp. Luminescence lifetimes in the infrared range were measured at 25 °C using a diode laser with an operating wavelength of 365 nm as an excitation source, an MDR-3 monochromator, a KS-19 filter, and an FEU-106 photomultiplier (the duration of laser pulse is < 2 μ s; the experimental accuracy $Dt_{1/2} = 5\%$). Photoluminescence quantum yields in the visible range were determined with the FluoroMax Plus spectrophotometer at room temperature according to an absolute method in the integration sphere. Photoluminescence quantum yield in the NIR range were determined with an Ocean Optics Maya 2000 spectrometer (Ocean Insight, USA) upon excitation with a xenon lamp at 25 °C ($\lambda_{\text{exc}} = 395$ nm). The absorption spectra of solutions in DMSO were recorded in the region 300–750 nm and 900–1100 nm with a Perkin-Elmer Lambda 35 spectrometer (Perkin Elmer Inc., USA). Pheophorbide *a* methyl ester was synthesized according to a previously described procedure.^[53]

22Rv1 human prostate carcinoma cells and MCF7 human breast adenocarcinoma cells were purchased from the American Type Culture Collection (ATCC, Manassas, VA, USA) and cultured in RPMI-1640 media (22Rv1) and EMEM (MCF7) (PanEco, Russia) supplemented with L-glutamine (PanEco, Russia), and 10% fetal calf serum (FCS, PanEco, Russia) in a 37 °C, 5% CO₂ atmosphere. All cell lines routinely tested negative for mycoplasma. Cells were seeded into 24-well plates in an amount of 10×10^3 per 1 mL. The test compounds were added to the wells 24 hours after seeding at a concentration of 0.05 μ M and incubated at 0.25; 1 and 3 hours, then the cells were washed with PBS to remove the added substances and fixed with a 4% formaldehyde solution. The accumulation and intracellular distribution of compounds 5–8 were studied on human prostate cell lines 22Rv1 and breast adenocarcinoma MCF7 using a laser scanning confocal microscope LSM-710 (Carl Zeiss, Jena, Germany), 10x Plan-Apochromat objective with a numerical aperture of 0.45 and ZEN 2010 software (Carl Zeiss, Jena, Germany). Fluorescence signals were recorded in the confocal channel mode with a confocal aperture diameter of 46 μ m and an image size of 2048×2048 pixels. Fluorescence was excited at $\lambda_{\text{exc}} = 633$ nm and recorded in the range $\lambda_{\text{em}} = 650$ –740 nm. The transmitted laser radiation was recorded by a separate T-PMT detector.

Synthesis

15,17-Dimethyl chlorin e₆ 13-N-(6-aminohexyl)amide (2). Pheophorbide *a* methyl ester (**1**) (100 mg, 0.165 mmol) was dissolved in CH₂Cl₂ (7 mL). Hexane-1,6-diamine (575 mg, 4.945 mmol) was added to the resulting solution. The reaction was performed for 3 h at 35 °C with stirring under argon atmosphere. After cooling the reaction mixture was diluted with CH₂Cl₂ (15 mL), washed

with saturated aqueous NaCl solution (5×20 mL), dried over anhydrous Na₂SO₄ and concentrated under reduced pressure. The target product was purified by column chromatography in a CH₂Cl₂/CH₃OH/NH₄OH eluent system (90/10/1, v/v). Yield: 119 mg (82 %). UV-Vis (CH₂Cl₂) λ_{max} nm (ϵ , M⁻¹ cm⁻¹): 405 (130,100), 501 (16,400), 528 (8,400), 556 (7,200), 607 (8,900), 663 (44,700). ¹H NMR (300 MHz, CDCl₃) δ ppm: 9.67 (H, s, 10-H), 9.63 (H, s, 5-H), 8.81 (H, s, 20-H), 8.06 (H, dd, $J = 17.8$ Hz, 11.5 Hz, 3¹-H), 6.55 (H, m, 13²-NH), 6.32 (H, d, $J = 17.8$ Hz, E-3²-H), 6.10 (H, d, $J = 11.5$ Hz, Z-3²-H), 5.54 (H, d, $J = 18.9$ Hz, 15-CH₂^a), 5.25 (H, d, $J = 19.0$ Hz, 15-CH₂^b), 4.47 (H, q, $J = 7.2$ Hz, 18-H), 4.34 (H, d, $J = 9.5$ Hz, 17-H), 3.79 (2H, m, 8¹-CH₂), 3.77 (3H, s, 15²-COOCH₃), 3.61 (3H, s, 12-CH₃), 3.51 (3H, s, 17³-COOCH₃), 3.48 (3H, s, 2-CH₃), 3.41 (2H, m, 13³-CH₂), 3.30 (3H, s, 7-CH₃), 2.84 (2H, m, 13⁸-CH₂), 2.55 (H, m, 17²-CH₂^a), 2.21 (H, m, 17¹-CH₂^a), 2.15 (H, m, 17²-CH₂^b), 1.77 (H, m, 17¹-CH₂^b), 1.73 (3H, d, $J = 7.1$ Hz, 18-CH₃), 1.68 (3H, t, $J = 7.6$ Hz, 8²-CH₃), 1.29 (8H, m, 13⁴-13⁷-CH₂), -1.86 (H, br.s, III - NH).

15,17-Dimethyl chlorin e₆ 13-N-(6-(bis(2-methoxy-2-oxoethyl)amino)hexyl)amide (3). Compound **2** (99 mg, 0.137 mmol) was dissolved in acetonitrile (10 mL). K₂CO₃ (84 mg, 0.608 mmol) and methyl bromoacetate (29 μ L, 0.306 mmol) was added to the resulting solution. The reaction was performed overnight at 25 °C with stirring under argon atmosphere. The reaction mixture was diluted with CH₂Cl₂ (15 mL), washed with water (3×20 mL), dried over anhydrous Na₂SO₄, and concentrated under reduced pressure. The target product was purified by column chromatography in a CH₂Cl₂-CH₃OH eluent system (50/1, v/v). Yield: 124 mg (72 %). UV-Vis (CH₂Cl₂) λ_{max} nm (ϵ , M⁻¹ cm⁻¹): 403 (130,000), 502 (16,400), 529 (8,400), 555 (7,300), 607 (9,000), 663 (44,800). ¹H NMR (300 MHz, CDCl₃) δ ppm: 9.70 (H, s, 10-H), 9.64 (H, s, 5-H), 8.81 (H, s, 20-H), 8.08 (H, dd, $J = 17.8$ Hz, 11.5 Hz, 3¹-H), 6.50 (H, m, 13²-NH), 6.35 (H, d, $J = 17.8$ Hz, E-3²-H), 6.14 (H, d, $J = 11.5$ Hz, Z-3²-H), 5.56 (H, d, $J = 18.9$ Hz, 15-CH₂^a), 5.27 (H, d, $J = 19.0$ Hz, 15-CH₂^b), 4.47 (H, q, $J = 7.2$ Hz, 18-H), 4.37 (H, d, $J = 9.5$ Hz, 17-H), 3.81 (2H, m, 8¹-CH₂), 3.79 (3H, s, 15²-COOCH₃), 3.61 (9H, s, 12-CH₃, N-CH₂-COOCH₃), 3.57 (3H, s, 17³-COOCH₃), 3.54 (3H, s, 2-CH₃), 3.51 (4H, s, N-CH₂-COOCH₃), 3.49 (2H, m, 13³-CH₂), 3.32 (3H, s, 7-CH₃), 2.74 (2H, m, 13⁸-CH₂), 2.53 (H, m, 17²-CH₂^a), 2.23 (H, m, 17¹-CH₂^a), 2.13 (H, m, 17²-CH₂^b), 1.81 (H, m, 17¹-CH₂^b), 1.75 (3H, d, $J = 7.1$ Hz, 18-CH₃), 1.73 (3H, t, $J = 7.6$ Hz, 8²-CH₃), 1.52 (8H, m, 13⁴-13⁷-CH₂), -1.58 (H, br.s, I - NH), -1.81 (H, br.s, III - NH).

Chlorin e₆ 13-N-(6-(bis(carboxymethyl)amino)hexyl)amide (4). Compound **3** (25 mg, 0.029 mmol) was dissolved in degassed acetone (1.5 mL), after which a solution of KOH (10 mg, 0.178 mmol) in degassed water (1.5 mL) was added to the mixture. The reaction was performed for 2 h at 50 °C. After cooling the reaction mixture was diluted with water (10 mL) and neutralized with 1N HCl and then evaporated. DMF was added to the evaporation residue containing the target product and NaCl, after which the mixture was decanted, and the solution of the target product was evaporated. Yield: 22 mg (95 %). UV-Vis (CH₂Cl₂) λ_{max} nm (ϵ , M⁻¹ cm⁻¹): 404 (130,300), 501 (16,400), 529 (8,400), 557 (7,300), 607 (9,100), 663 (44,700). ESI MS m/z calculated for C₄₄H₅₄N₆O₉ [M]⁺: 810.3952; Found: 810.3945. ¹H NMR (300 MHz, DMSO- d_6) δ ppm: 9.76 (2H, s, 10-H, 5-H), 9.14 (2H, s, 20-H, 13²-NH), 8.33 (H, dd, $J = 17.8$ Hz, 11.5 Hz, 3¹-H), 6.45 (H, d, $J = 17.8$ Hz, E-3²-H), 6.17 (H, d, $J = 11.5$ Hz, Z-3²-H), 5.46 (H, d, $J = 18.9$ Hz, 15-CH₂^a), 5.29 (H, d, $J = 19.0$ Hz, 15-CH₂^b), 4.62 (H, q, $J = 7.2$ Hz, 18-H), 4.39 (H, d, $J = 9.5$ Hz, 17-H), 3.82 (2H, m, 8¹-CH₂), 3.66 (3H, s, 12-CH₃), 3.53 (3H, s, 2-CH₃), 3.49 (4H, s, N-CH₂-COOH), 3.41 (2H, m, 13³-CH₂), 3.31 (3H, s, 7-CH₃), 2.84 (2H, m, 13⁸-CH₂), 2.63 (H, m, 17²-CH₂^a), 2.30 (H, m, 17¹-CH₂^a), 2.14 (H, m, 17²-CH₂^b), 1.80 (H, m, 17¹-CH₂^b), 1.67 (3H, t, $J = 7.6$ Hz, 8²-CH₃), 1.62 (3H, d, $J = 7.1$ Hz, 18-CH₃), 1.49 (8H, m, 13⁴-13⁷-CH₂), -1.89 (H, br.s, I - NH), -2.21 (H, br.s, III - NH).

*15,17-Dimethyl chlorin e₆ 13-N-(6-(bis(2-*tert*-butoxy)-2-oxoethyl)amino)hexyl)amide (6)*. Compound **3** (150 mg, 0.207 mmol) was dissolved in CH₂Cl₂ (2 mL), after which di-*tert*-

butyl 2,2'-((2-bromoethyl)azanediy)diacetate (560 mg, 1.590 mmol) and anhydrous K_2CO_3 (55 mg, 0.398 mmol) were added to the resulting solution. The reaction was performed for 24 h at room temperature. The reaction mixture was diluted with CH_2Cl_2 (10 mL), washed with water (3×20 mL), dried over anhydrous Na_2SO_4 , and concentrated under reduced pressure. The target product was purified by column chromatography in a CH_2Cl_2 - CH_3OH eluent system (25/1, v/v). Yield: 215 mg (85%). UV-Vis (CH_2Cl_2) λ_{max} nm (ϵ , $M^{-1}cm^{-1}$): 403 (130,100), 501 (16,400), 529 (8,400), 556 (7,300), 608 (9,000), 664 (44,500). ESI MS m/z calculated for $C_{70}H_{104}N_8O_{13}$ $[M+H]^+$: 1264.77; $[M+2H]^{2+}$: 632.39. Found: 1265.77; 633.39. 1H NMR (300 MHz, $CDCl_3$) δ ppm: 9.70 (H, s, 10-H), 9.63 (H, s, 5-H), 8.80 (H, s, 20-H), 8.08 (H, dd, $J = 17.9$ Hz, 11.7 Hz, 3¹-H), 6.60 (H, m, 13²-NH), 6.34 (H, d, $J = 17.7$ Hz, E-3²-H), 6.13 (H, d, $J = 11.6$ Hz, Z-3²-H), 5.55 (H, d, $J = 18.8$ Hz, 15-CH₂^a), 5.26 (H, d, $J = 19.0$ Hz, 15-CH₂^b), 4.47 (H, q, $J = 7.6$ Hz, 18-H), 4.36 (H, d, $J = 8.5$ Hz, 17-H), 3.80 (3H, s, 15³-CO₂CH₃), 3.80 (2H, m, 8¹-CH₂), 3.60 (3H, s, 17⁴-CO₂CH₃), 3.57 (3H, s, 12³-CH₃), 3.49 (3H, s, 2-CH₃), 3.44 (8H, s, 4CH₂COO), 3.32 (3H, s, 7-CH₃), 3.11 (2H, m, N-CH₂), 2.54 (2H, m, 17²-CH₂), 2.18 (2H, m, 17¹-CH₂), 1.82 (3H, m, 18-CH₃), 1.73 (3H, t, $J = 7.7$ Hz, 8²-CH₃), 1.63–1.48 (6H, m, CH₂-CH₂-N, N-CH₂), 1.44 (36H, s, O⁻¹Bu), 1.36–1.21 (4H, m, CH₂-CH₂), -1.81 (H, br.s, NH), -1.82 (H, br.s, NH).

15,17-Dimethyl chlorin e₆ 13-N-(6-(bis(2-(bis(carboxymethyl)amino)ethyl)amino)hexyl)amide (7). Compound **6** (100 mg, 0.079 mmol) was dissolved in a 20% solution of TFA in CH_2Cl_2 (3 mL). The reaction was performed for 3 h at room temperature. The reaction mixture was diluted with CH_2Cl_2 (10 mL), washed with 10 % aqueous $NaHCO_3$ solution (3·20 mL), dried over anhydrous Na_2SO_4 , and concentrated under reduced pressure. The target product was purified by column chromatography in a CH_2Cl_2 - CH_3OH eluent system (20/1, v/v). Yield: 78 mg (95%). UV-Vis (CH_2Cl_2) λ_{max} nm (ϵ , $M^{-1}cm^{-1}$): 403 (130,100), 501 (16,400), 529 (8,400), 556 (7,300), 607 (9,000), 663 (44,700). ESI MS m/z calculated for $C_{54}H_{72}N_8O_{13}$ $[M+H]^+$: 1040.52; $[M+2H]^{2+}$: 520.7. Found: 1041.53; 521.27. 1H NMR (300 MHz, DMSO- d_6) δ ppm: 9.85 (H, s, 10-H), 9.82 (H, s, 5-H), 9.17 (H, s, 20-H), 8.33 (H, dd, $J = 17.8$, 11.6 Hz, 3¹-H),), 7.75 (H, m, 13²-NH), 6.47 (H, d, $J = 17.8$ Hz, E-3²-H), 6.21 (H, d, $J = 11.6$ Hz, Z-3²-H), 5.54 (2H, d, $J = 18.8$ Hz, 15-CH₂^a), 5.33 (2H, d, $J = 18.9$ Hz, 15-CH₂^b), 4.62 (H, m, 18-H), 4.43 (H, d, $J = 9.9$ Hz, 17-H), 3.85 (5H, m, 15³-CO₂CH₃, 8¹-CH₂), 3.68 (3H, s, 17⁴-CO₂CH₃), 3.54 (14H, m, 12³-CH₃, 2-CH₃, 4CH₂COO), 3.34 (3H, s, 7¹-CH₃), 3.09 (4H, m, N-CH₂, 17²-CH₂), 1.81 (2H, m, 17¹-CH₂), 1.67 (6H, m, 18¹-CH₃, 8²-CH₃), 1.24 (10H, m, CH₂-CH₂-N, N-CH₂, CH₂-CH₂), -1.96 (H, s, NH), -2.15 (H, s, NH).

Preparation of the ytterbium complex of compound 4 (5). Compound **4** (26 mg, 0.03 mmol) was suspended in water (50 mL) followed by the addition of potassium hydroxide (7 mg, 0.12 mmol). After complete dissolution of the precipitate, $YbCl_3$ (17 mg, 0.04 mmol) was added. The solution was then stirred for 2 hours at a room temperature. The formed precipitate was centrifuged and washed with water to remove traces of soluble impurities. The precipitate was dried and complex **5** was obtained as black powder. Yield: 30 mg (93%). UV-Vis (DMSO) λ_{max} nm (ϵ , $M^{-1}cm^{-1}$): 406 (126,200), 501 (16,700), 532 (8,000), 557 (7,200), 607 (9,000), 664 (44,100).

Preparation of the ytterbium complex of compound 7 (8). The procedure is similar to the method described for compound **5**. Starting from compound **7** (11 mg; 0.01 mmol) we obtained 4.5 mg of **8** (37.5%). UV-Vis (DMSO) λ_{max} nm (ϵ , $M^{-1}cm^{-1}$): 405 (125,900), 505 (15,600), 530 (8,500), 559 (7,000), 614 (7,900), 667 (43,800). MALDI MS m/z calculated for $C_{54}H_{68}N_8O_{13}Yb$ $[M]^+$: 1213.45; $[M-N((CH_2)_2-N(CH_2COOH)_2)]^{2+}$: 450.73. Found: 451.43.

Results and Discussion

The starting material for the synthesis of chelators was pheophorbide *a* methyl ester (**1**), which was treated with an excess of 1,6-diaminohexane in DCM, which led to the opening of exocycle E and the formation of chlorin **2** containing a terminal amino group. The resulting aminoamide was alkylated with methyl bromoacetate in the presence of potassium carbonate to form compound **3**. In the 1H NMR spectrum, signals from methyl groups in the iminodiacetic fragment were detected. During the alkaline hydrolysis of compound **3** under the action of potassium hydroxide, the removal of methyl groups was observed both in the chelating fragment and in positions 15² and 17³ of the chlorin macrocycle, which was confirmed by the disappearance of the corresponding signals in the 1H NMR spectrum. A molecular ion corresponding to that expected for product **4** was detected in the high-resolution mass spectrum. The resulting chlorin derivative had high solubility in aqueous solutions, both at acidic and alkaline pH values. For this reason, to separate it from the potassium chloride formed after neutralization, the reaction mass was dried and then redissolved in DMF, followed by filtering the chlorin solution from the inorganic salt. Thus, a water-soluble photosensitizer was obtained containing fragments of chlorin and iminodiacetic acid, separated by a spacer group. In order to increase the chelating ability, a derivative containing a larger number of nitrogen atoms and carboxyl groups in the complexing fragment was also obtained. For this purpose, aminoamide **2** was treated with di-*tert*-butyl 2,2'-((2-bromoethyl)azanediy)diacetate in a basic medium to obtain chlorin **6**. In the 1H NMR spectrum of compound **6**, signals of *tert*-butyl groups, as well as methylene units in the composition of iminodiacetic acid fragments. Removal of *tert*-butyl groups was carried out by acidolysis using trifluoroacetic acid. The resulting carboxylate derivative **7** had excellent solubility in aqueous media with $pH > 7$, and was also soluble at $pH < 3$, which was apparently due to the presence of methyl groups in the chlorin macrocycle.

Ytterbium complexes of compounds **4** and **7** were obtained by the interaction of freshly prepared potassium salt of the ligand and ytterbium chloride in the aqueous solution. Potassium salt of the ligand was preliminarily obtained, a weighed portion of the ligand was suspended at a room temperature and constant stirring in an aqueous solution and aqueous solution of KOH was added. After complete dissolution of the ligand, ytterbium chloride $YbCl_3$ was added to it. The solution was then stirred for 2 h at a room temperature. The formed precipitate was centrifuged and washed with water to remove traces of soluble impurities. The precipitates were dried in air for 7 days. Black powders of complexes **5** and **8** were obtained. The resulting ytterbium complexes were characterized by NMR spectroscopy and MALDI mass spectrometry, as well as luminescence spectroscopy and spectrophotometry.

Mass-spectrometry is a powerful method to analyze the lanthanide complexes due to the specific isotopic distribution of lanthanide ions. This allows securely distinguish between Ln-free and Ln-containing species, as well as to verify the presence of oligonuclear species. In the MALDI

MS spectra of **5**, the most intense signal, corresponding to the $\text{Yb}(\text{L}^1)^{2+}$ species, was detected within the $m/z=440\text{--}460$ range, as during the ionization of the investigated substance the elimination of $-\text{CH}_2\text{COOH}$ group occurs. In the MALDI MS spectra of **8**, the most intense signals correspond to the different eliminated groups of ligand, but the band within the $m/z = 440\text{--}460$ range can also be found, corresponding to the $\text{Yb}(\text{L}^2)^{2+}$ species with the eliminated $\text{N}((\text{CH}_2)_2\text{-N}(\text{CH}_2\text{COOH})_2)_2$ group. The intensities ratio of these bands for each ytterbium complex corresponds to the theoretical isotopic distribution, calculated for these complexes. The high intensity of the signal corresponding to complex $\text{Yb}(\text{L}^1)^{2+}$ in comparison with $\text{Yb}(\text{L}^2)^{2+}$ may be due to the presence of two carboxy-groups attached to the aromatic system rather than to

the aliphatic fragment. If the aliphatic fragment is eliminated under the ionizing radiation (its bands are present in the spectrum), ytterbium will be coordinated by these carboxylic groups, which are not present in complex $\text{Yb}(\text{L}^2)^{2+}$.

^1H NMR spectroscopy is also very informative method for the analysis of lanthanide complexes. In the present case, the reason for that lays in the fact that paramagnetic central ion results in the lanthanide-induced shift (LIS) and broadening, allowing to not only proof the complex formation, but also to get some information about its geometry.^[54,55] The ^1H NMR spectra in $\text{DMSO-}d_6$ show the signals from ligands, that are broadened and shifted in accordance with the paramagnetic ion effect (Figure 1), which confirms the formation of the ytterbium complex.

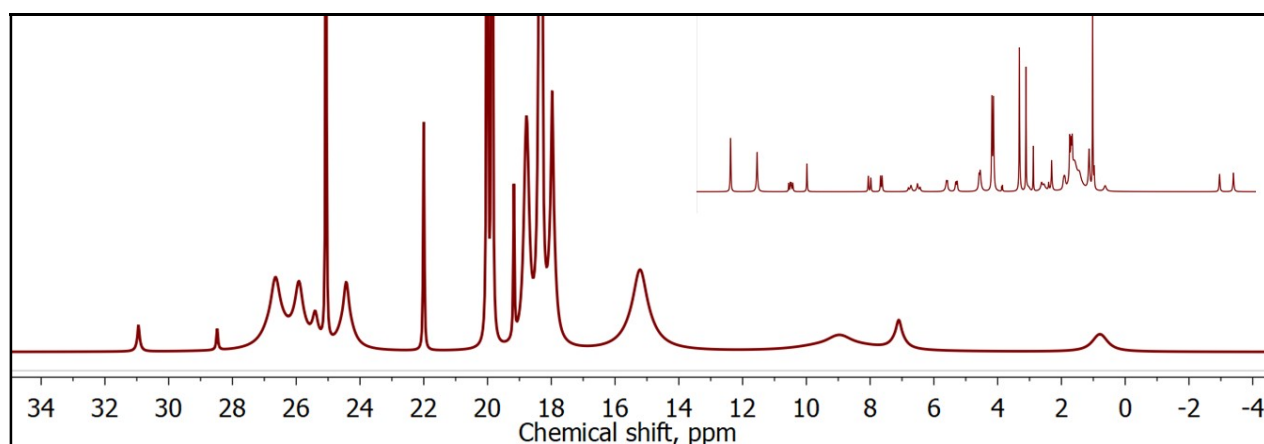
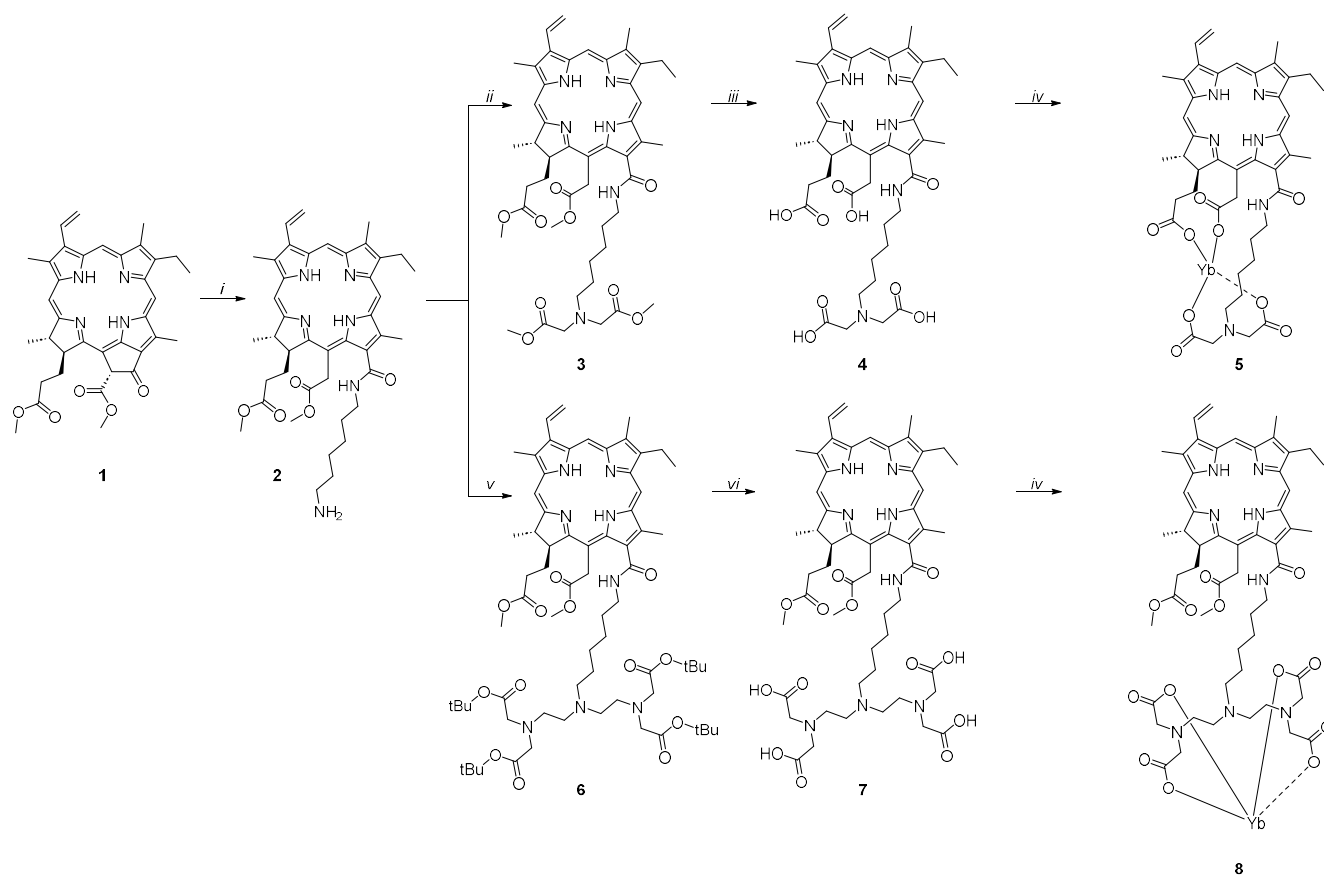


Figure 1. ^1H NMR spectra of **5** and **4** (inset) in $\text{DMSO-}d_6$.

Infrared luminescence of ytterbium complexes **5** and **8** was studied upon through-ligand excitation (Figure 2) and demonstrated typical Yb^{3+} ion emission, corresponding to ${}^2\text{F}_{7/2} \rightarrow {}^2\text{F}_{5/2}$ transition (Figure 2). Quantum yields (QY) of **5** and **8** solutions in $\text{DMSO-}d_6$ reached 0.14% and 0.09%, respectively (Table 1).

To understand the factor limiting quantum yield values, we separately calculated sensitization efficiency η_{sens} and internal quantum yield $\text{QY}_{\text{Yb}}^{\text{Yb}}$, which product is the overall quantum yield $\text{QY}_{\text{Yb}}^{\text{L}} = \eta_{\text{sens}} \cdot \text{QY}_{\text{Yb}}^{\text{Yb}}$. Internal quantum yield equals the ratio between observed and radiative lifetimes $\text{QY}_{\text{Yb}}^{\text{Yb}} = \tau_{\text{obs}}/\tau_{\text{rad}}$, where observed lifetime was experimentally determined in solution from the luminescence decay curves to be 7 μs and 38 μs for **5** and **8** respectively

(Table 1). Radiative lifetime cannot be determined directly, but for ytterbium complexes it can be calculated from the absorption spectrum corresponding to the ytterbium emission spectrum with the help of the modified Einstein's equation:

$$\frac{1}{\tau_{\text{rad}}} = 2303 \times \frac{8\pi c n^2 \bar{\nu}_{ul}^2 (2J+1)}{N_A (2J'+1)} \int \varepsilon(\nu) d\nu,$$

where c is the speed of light in vacuum (cm/s), n is refractive index, N_A is Avogadro constant, J and J' are the quantum numbers of the ground and excited states, respectively, $\int \varepsilon(\nu) d\nu$ is the integrated spectrum of the f-f transition, and $\bar{\nu}_{ul}^2 = \frac{\int \nu \varepsilon(\nu) d\nu}{\int \varepsilon(\nu) d\nu}$ is the barycentre of the transition.

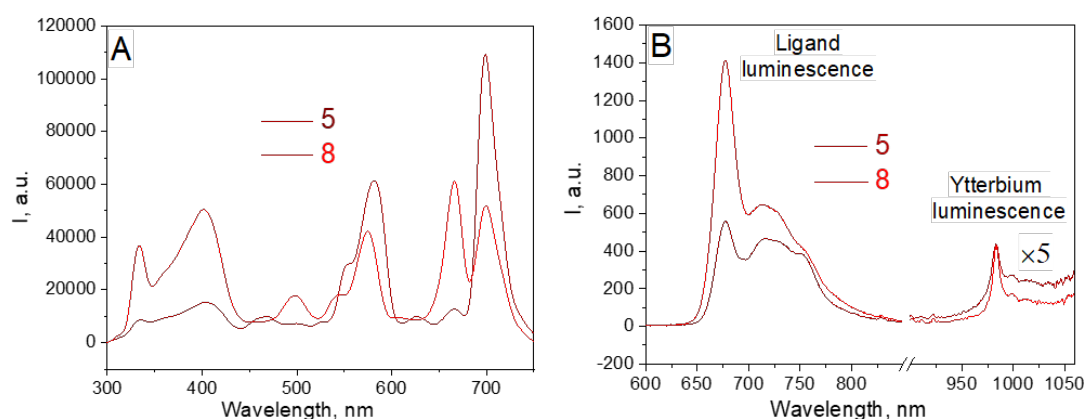


Figure 2. Excitation (A) ($\lambda_{\text{em}} = 670 \text{ nm}$) and emission (B) spectra of complexes **5** and **8** solutions in $\text{DMSO-}d_6$ ($C = 4 \text{ mmol/L}$). The intensity of ytterbium luminescence bands is increased by 5 times.

Table 1. Overall quantum yields, radiative (τ_{rad}), and observed (τ_{obs}) luminescence lifetimes of ytterbium ions luminescence for studied complexes.

Compound	$\text{QY}_{\text{Yb}}^{\text{L}}, \%$	$\text{QY}_{\text{Yb}}^{\text{Yb}}, \%$	$\tau_{\text{rad}}(\text{Yb}), \text{ms}$	$\tau_{\text{obs}}(\text{Yb}), \mu\text{s}$	$\text{QY}_{\text{Yb}}^{\text{Yb}}, \%$	$\eta_{\text{sens}}(\text{L-Yb}), \%$
5	0.14	2.04	0.07	7	10.8	1.30
8	0.09	3.55	0.07	38	55.9	0.16

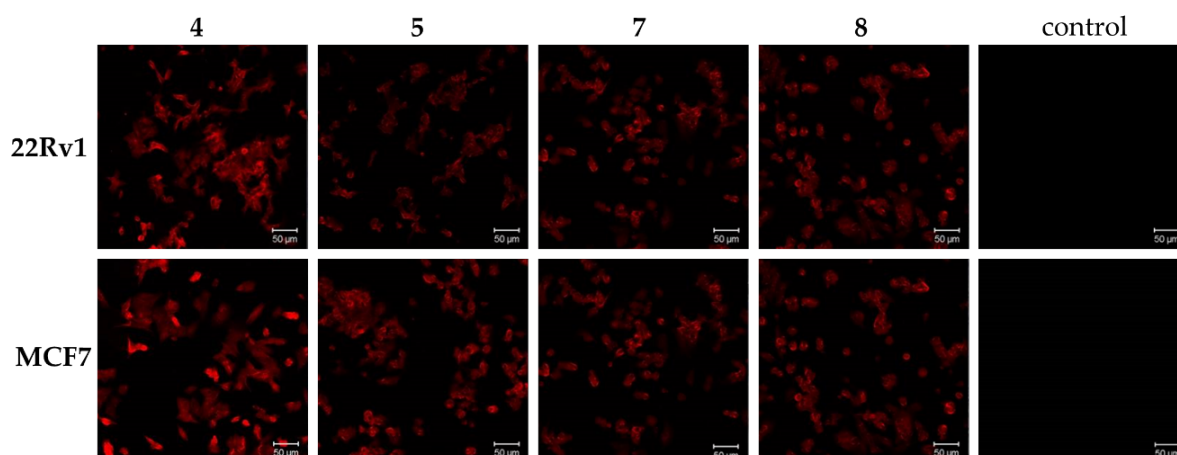


Figure 3. Fluorescent microscopy images of 22Rv1 prostate carcinoma cells and MCF7 breast adenocarcinoma cells after 3-hour incubation with compounds **4**, **5**, **7** and **8**; control – cells without treatment.

Radiative lifetime in DMSO- d_6 is equal to 0.07 ms for both complexes **5** and **8** (Table 1). The internal quantum yields reach 10.8% for **5** and 55.9% for **8**, which is rather high for infrared luminescence. The sensitization efficiency values of ytterbium ion are rarely reported in the literature, and though among published the high value can be found, usually these values do not exceed several percent, if published. Thus, the limiting factor was the sensitization efficiency, which equals 1.3% for **5** and 0.16% for **8**.

Cancer diagnostic applications demand high luminosity, which is equal to the multiplication of the molar absorption coefficient and the quantum yield. Despite the not the highest quantum yields of ytterbium, we obtain high luminosity values due to high absorption. In combination with the vector properties of our ligands, this makes our complexes promising for applications as luminescent bioprobes.

The properties of the obtained derivatives allow the use of fluorescence microscopy to study the interaction of these compounds with tumor cells. It was found that all studied compounds **4**, **5**, **7**, **8** accumulate in 22Rv1 prostate carcinoma and MCF7 breast adenocarcinoma cells after 15 min of incubation; maximum accumulation was observed after 1–3 h (Figures 3, S6, S7). The dyes were diffusely distributed in the cytoplasmic region. To study the dynamics of accumulation of the resulting metal complexes **5**, **8**, as well as the initial photosensitizers **4**, **7**, fluorescence intensity calculations were made in tumor cells. The results of the study are presented in Figure 4. In the case of complex **5**, a decrease in the accumulation rate was observed compared to metal-free PS **4** in both the cell lines. Thus, in 22Rv1 cells, the rate of accumulation of compound **5** was 2

times slower than for the original photosensitizer. In MCF7 cells, the accumulation of compounds **4** and **5** after 3 h was almost the same, but at lower times there was a tendency for the penetration rate of the metal complex into the cells to decrease. In contrast, when studying the dynamics of accumulation of pigment **7** and its Yb-complex **8**, improved cellular uptake of the latter was observed. This circumstance can be explained by the presence of ester groups in complex **8**, which do not participate in the coordination of the ytterbium atom, in contrast to complex **5**, which contains carboxyl groups at positions **15** and **17** of the chlorin macrocycle. Apparently, the participation of these carboxyl groups in complex formation significantly affects the ability of chlorins to penetrate into tumor cells.

Conclusions

For the first time, chlorin e_6 derivatives containing iminodiacetic acid residues for chelation of lanthanides were synthesized. In this work, Yb complexes were prepared and long lifetimes and high quantum yields of infrared luminescence were demonstrated. It was established that the target compounds obtained in the work penetrate and accumulate in 22Rv1 prostate carcinoma and MCF7 breast adenocarcinoma cells after 15 minutes of incubation. The most intense accumulation of these compounds occurs 1–3 hours after the start of incubation, which is typical for chlorin derivatives. Due to the photophysical properties of the obtained ytterbium chlorin complexes, they have diagnostic potential as luminescent bioprobes.

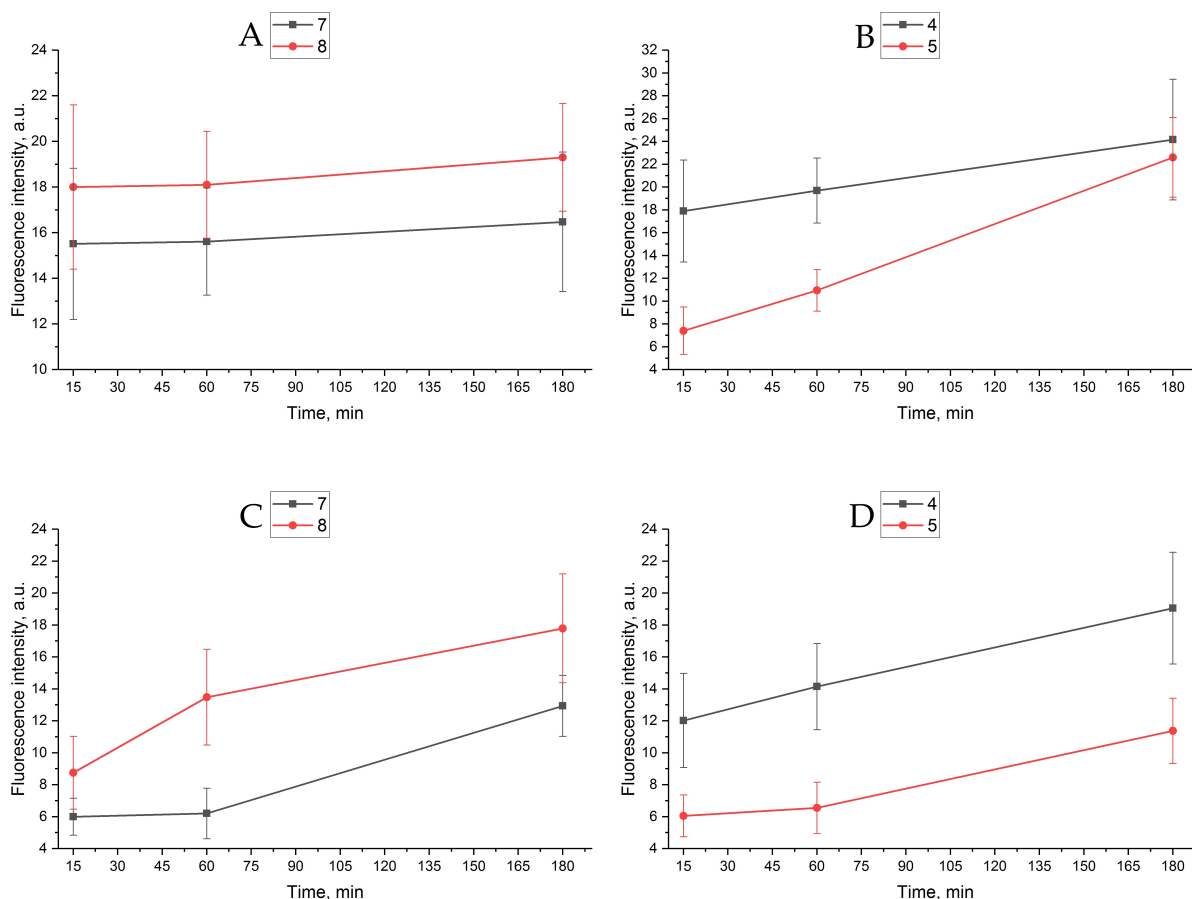


Figure 4. Accumulation kinetics of photosensitizers **4**, **5**, **7**, **8** in 22Rv1 (A, B) and MCF7 (C, D) cell lines.

Acknowledgements. The study was supported by Ministry of Science and Higher Education of the Russian Federation (FSFZ-2023-0004). This work was performed using the equipment of the Shared Science and Training Centre for Collective Use RTU MIREA and supported by the Ministry of Science and Higher Education of the Russian Federation within the framework of agreement No. 075-15-2021-689 dated 01.09.2021. The part of this work was carried out within the State Program of TIPS RAS.

Supplementary Materials. NMR data for synthesized chlorins and fluorescent micrographs of 22Rv1 and MCF7 cells are available online as separate file.

Author Contributions. Alexander A. Popov: investigation, writing - original draft, visualization; Nikita V. Suvorov: investigation, validation, writing - original draft; Andrey I. Kornikov: investigation, writing - original draft, visualization; Petr V. Ostroverkhov: investigation, validation; Sergey I. Tikhonov: investigation, formal analysis; Viktor A. Pogorilyy: investigation, formal analysis; Anastasia I. Demina: investigation; Maxim N. Usachev: investigation, visualization; Ekaterina A. Plotnikova: investigation, writing - original draft; Andrey A. Pankratov: validation, formal analysis, resources, writing - review & editing; Leonid S. Lepnev: investigation, visualization; Elnara S. Saffiulina: investigation; Valentina V. Utochnikova: conceptualization, validation, writing - review & editing, supervision; Elena R. Milaeva: conceptualization, validation, writing - review & editing; Mikhail A. Grin: conceptualization, resources, writing - review & editing, project administration, funding acquisition. Please, Insert each author's contribution.

References

1. Glunde K., Jacobs M.A., Pathak A.P., Artemov D., Bhujwalla Z.M. *NMR Biomed.* **2009**, *22*, 92–103. DOI: 10.1002/nbm.1269.
2. Bünzli J.C.G. *Chem. Lett.* **2009**, *38*, 104–109. DOI: 10.1246/cl.2009.104.
3. Bünzli J.C.G. *Chem. Rev.* **2010**, *110*, 2729–2755. DOI: 10.1021/cr900362e.
4. Fang H., Chen Y., Jiang Z., He W., Guo Z. *Acc. Chem. Res.* **2023**, *56*, 258–269. DOI: 10.1021/acs.accounts.2c00643.
5. Wang R., Zhang F. *J. Mater. Chem. B* **2014**, *2*, 2422–2443. DOI: 10.1039/C3TB21447H.
6. Weissleder R. *Nat. Biotechnol.* **2001**, *19*, 316–317. DOI: 10.1038/86684.
7. König K. *J. Microsc.* **2000**, *200*, 83–104. DOI: 10.1046/j.1365-2818.2000.00738.x.
8. Ning Y., Chen S., Chen H., Wang J.X., He S., Liu Y.W., Cheng Z., Zhang J.L. *Inorg. Chem. Front.* **2019**, *6*, 1962–1967. DOI: 10.1039/C9QI00157C.
9. Ning Y., Tang J., Liu Y.W., Jing J., Sun Y., Zhang J.L. *Chem. Sci.* **2018**, *9*, 3742–3753. DOI: 10.1039/C8SC00259B.
10. Kovalenko A.D., Pavlov A.A., Ustinovich I.D., Kalyakina A.S., Goloveshkin A.S., Marciniak Ł., Lepnev L.S., Burlov A.S., Schepers U., Bräse S., Utochnikova V.V. *Dalton Trans.* **2021**, *50*, 3786–3791. DOI: 10.1039/D0DT03913F.
11. Get'man E.I., Oleksii Y.A., Radio S.V., Ardanova L.I. *Fine Chemical Technologies* **2020**, *15*, 54–62. DOI: 10.32362/2410-6593-2020-15-5-54-62.
12. D'Aléo A., Bourdolle A., Brustlein S., Fauquier T., Grichine A., Duperray A., Baldeck P.L., Andraud C., Brasselet S., Maury O. *Angew. Chemie* **2012**, *124*, 6726–6729. DOI: 10.1002/anie.201202212.
13. Khan Y., Han D., Pierre A., Ting J., Wang X., Lochner C.M., Bovo G., Yaacobi-Gross N., Newsome C., Wilson R., Arias A.C. *Proc. Natl. Acad. Sci. U. S. A.* **2018**, *115*, E11015–E11024. DOI: 10.1073/pnas.1813053115.
14. He M., Ye M., Li B., Wu T., Lu C., Liu P., Li H., Zhou X., Wang, Y., Liang, T., Li H., Li Ch. *Sens. Actuators, B* **2022**, *364*, 131868. DOI: 10.1016/j.snb.2022.131868.
15. Yan Y., Li S., Zhang Z.H., Qu J., Wang J.Y. *Spectrochim. Acta - Part A Mol. Biomol. Spectrosc.* **2021**, *260*, 119988. DOI: 10.1016/j.saa.2021.119988.
16. Bünzli J.-C.G., Eliseeva S.V. Basics of Lanthanide Photophysics. In: *Lanthanide Luminescence. Springer Series on Fluorescence, Vol. 7* (Hänninen P., Härmä H., Eds.), Springer, Berlin, Heidelberg, **2010**. pp. 1–45. DOI: 10.1007/4243_2010_3.
17. Bünzli J.-C.G. *Coord. Chem. Rev.* **2015**, *293–294*, 19–47. DOI: 10.1016/j.ccr.2014.10.013.
18. Sy M. *Chem. Commun.* **2016**, *52*, 5080–5095. DOI: 10.1039/C6CC00922K.
19. Berezin M.Y., Achilefu S. *Chem. Rev.* **2010**, *110*, 2641–2684. DOI: 10.1021/cr900343z.
20. Wu F., Yue L., Yang L., Wang K., Liu G., Luo X., Zhu X. *Colloids Surf., B* **2019**, *175*, 272–280. DOI: 10.1016/j.colsurfb.2018.11.054.
21. Dasari S., Singh S., Kumar P., Sivakumar S., Patra A.K. *Eur. J. Med. Chem.* **2019**, *163*, 546–559. DOI: 10.1016/j.ejmech.2018.12.010.
22. Cable M.L., Levine D.J., Kirby J.P., Gray H.B., Ponce A. *Adv. Inorg. Chem.* **2011**, *63*, 1–45. DOI: 10.1016/B978-0-12-385904-4.00010-X.
23. Ke X.S., Yang B.Y., Cheng X., Chan S.L.F., Zhang J.L. *Chem. Eur. J.* **2014**, *20*, 4324–4333. DOI: 10.1002/chem.201303972.
24. Bulach V., Sguerra F., Hosseini M.W. *Coord. Chem. Rev.* **2012**, *256*, 1468–1478. DOI: 10.1016/j.ccr.2012.02.027.
25. Hu J.Y., Ning Y., Meng Y.S., Zhang J., Wu Z.Y., Gao S., Zhang J.L. *Chem. Sci.* **2017**, *8*, 2702–2709. DOI: 10.1039/C6SC05021B.
26. Sekhosana K.E., Nyokong T. *Opt. Mater. (Amst)*. **2014**, *37*, 139–146. DOI: 10.1016/j.optmat.2014.05.013.
27. Gerasymchuk Y., Tomachynski L., Guzik M., Koll A., Jański J., Guyot Y., Stręk W., Boulon G., Legendziewicz J. *J. Photochem. Photobiol. A Chem.* **2015**, *309*, 65–71. DOI: 10.1016/j.jphotochem.2015.04.022.
28. Erzunov D., Sarvin I., Belikova A., Vashurin A. *Molecules* **2022**, *27*, 4050. DOI: 10.3390/molecules27134050.
29. Li B.Y., Yao Y.M., Wang Y.R., Zhang Y., Shen Q. *Polyhedron* **2008**, *27*, 709–716. DOI: 10.1016/j.poly.2007.10.025.
30. Koshelev D.S., Tcelykh L.O., Mustakimov R.E., Medved'ko A.V., Latipov E.V., Pavlov A.A., Goloveshkin A.S., Gontcharenko V.E., Vlasova K.Y., Burlov A.S., Lepnev L.S., Vatsadze S.Z., Utochnikova V.V. *J. Lumin.* **2023**, *263*, 120054. DOI: 10.1016/j.jlumin.2023.120054.
31. Kornikov A.I., Mustakimov R.E., Goloveshkin A.S., Tcelykh L.O., Vashchenko A.A., Medvedko A.V., Lepnev L.S., Utochnikova V.V. *Org. Electron.* **2022**, *105*, 106492. DOI: 10.1016/j.orgel.2022.106492.
32. Han F., Teng Q., Zhang Y., Wang Y., Shen Q. *Inorg. Chem.* **2011**, *50*, 2634–2643. DOI: 10.1021/ic102529d.
33. Utochnikova V.V., Kalyakina A.S., Bushmarinov I.S., Vashchenko A.A., Marciniak Ł., Kaczmarek A.M., Van Deun R., Bräse S., Kuzmina N.P. *J. Mater. Chem. C* **2016**, *4*, 9848–9855. DOI: 10.1039/C6TC03586H.
34. Faulkner S., Pope S.J.A., Burton-Pye B.P. *Appl. Spectrosc. Rev.* **2005**, *40*, 1–31. DOI: 10.1081/ASR-200038308.

35. Kornilov A.D., Grigoriev M.S., Savinkina E.V. *Fine Chemical Technologies* **2022**, *17*, 172–181. DOI: 10.32362/2410-6593-2022-17-2-172-181.
36. Li Z.-Y., Shi Y.-L., Liang G.-X., Yang J., Zhuang S.-K., Lin J.-B., Ghodbane A., Tam M.-S., Liang Z.-J., Zha Z.-G., Zhang H.-T. *ACS Omega* **2020**, *5*, 15911–15921. DOI: 10.1021/acsomega.0c01054.
37. Numasawa K., Hanaoka K., Saito N., Yamaguchi Y., Ikeno T., Echizen H., Yasunaga M., Komatsu T., Ueno T., Miura M., Nagano T., Urano Y. *Angew. Chem. Int. Ed.* **2020**, *59*, 6015–6020. DOI: 10.1002/ange.201914826.
38. Pourmadadi M., Mahdi Eshaghi M., Ostovar S., Mohammadi Z., Sharma R.K., Paiva-Santos A.C., Rahmani E., Rahdar A., Pandey S. *J. Drug Deliv. Sci. Technol.* **2023**, *82*, 104357. DOI: 10.1016/j.jddst.2023.104357.
39. Tazawa H., Shigeyasu K., Noma K., Kagawa S., Sakurai F., Mizuguchi H., Kobayashi H., Imamura T., Fujiwara T. *Cancer Sci.* **2022**, *113*, 1919–1929. DOI: 10.1111/cas.15369.
40. Hoffman R.M. *Lab. Investig.* **2015**, *95*, 432–452. DOI: 10.1038/labinvest.2014.154.
41. Dammes N., Peer D. *Theranostics* **2020**, *10*, 938–955. DOI: 10.7150/thno.37443.
42. Nikfarjam Z., Zargari F., Nowroozi A., Bavi O. *Biophys. Rev.* **2022**, *14*, 303–315. DOI: 10.1007/s12551-021-00919-1.
43. Celli J.P., Spring B.Q., Rizvi I., Evans C.L., Samkoe K.S., Verma S., Pogue B.W., Hasan T. *Chem. Rev.* **2010**, *110*, 2795–2838. DOI: 10.1021/cr900300p.
44. Akopov A., Rusanov A., Gerasin A., Kazakov N., Urtenova M., Chistyakov I. *Photodiagn. Photodyn. Ther.* **2014**, *11*, 259–264. DOI: 10.1016/j.pdpdt.2014.03.011.
45. Suvorov N., Pogorilyy V., Diachkova E., Vasil'ev Y., Mironov A., Grin M. *Int. J. Mol. Sci.* **2021**, *22*, 6392. DOI: 10.3390/ijms22126392.
46. Grin M.A., Suvorov N.V., Mironov A.F. *Mendeleev Commun.* **2020**, *30*, 406–418. DOI: 10.1016/j.mencom.2020.07.003
47. Gouterman M. *J. Mol. Spectrosc.* **1961**, *6*, 138–163. DOI: 10.1016/0022-2852(61)90236-3.
48. Rabinowitch E. *Rev. Mod. Phys.* **1944**, *16*, 226. DOI: 10.1103/RevModPhys.16.226.
49. Aita K., Temma T., Kuge Y., Seki K.I., Saji H. *Luminescence* **2010**, *25*, 19–24. DOI: 10.1002/bio.1136.
50. Faulkner S., Pope S.J.A. *J. Am. Chem. Soc.* **2003**, *125*, 10526–10527. DOI: 10.1021/ja035634v.
51. Zhao X., Zhuo R., Lu Z., Liu W. *Polyhedron* **1997**, *16*, 2755–2759. DOI: 10.1016/S0277-5387(97)00029-6.
52. Janicki R., Starynowicz P., Mondry A. *Eur. J. Inorg. Chem.* **2008**, *2008*, 3075–3082. DOI: 10.1002/ejic.200800249.
53. Jinadasa R.G.W., Hu X., Vicente M.G.H., Smith K.M. *J. Med. Chem.* **2011**, *54*, 7464–7476. DOI: 10.1021/jm2005139.
54. Parker D., Suturina E.A., Kuprov I., Chilton N.F. *Acc. Chem. Res.* **2020**, *53*, 1520–1534. DOI: 10.1021/acs.accounts.0c00275.
55. Forsberg J.H. Chapter 153 NMR studies of paramagnetic lanthanide complexes and shift reagents. In: *Handbook on the Physics and Chemistry of Rare Earths* (Gschneidner K.A., Jr., Eyring L.R., Eds.), **1996**, *23*, pp. 1–68. DOI: 10.1016/S0168-1273(96)23004-1.

Received 07.07.2024

Accepted 04.10.2024